J|A|C|S
ARTICLES
Published on Web 08/01/2006

Molecular Dynamics Simulations on the *Escherichia coli* Ammonia Channel Protein AmtB: Mechanism of Ammonia/Ammonium Transport

Yuchun Lin,[†] Zexing Cao,[‡] and Yirong Mo*[,†,‡]

Contribution from the Department of Chemistry, Western Michigan University, Kalamazoo, Michigan 49008, and Department of Chemistry, The State Key Laboratory for Physical Chemistry of Solid States, Center for Theoretical Chemistry, Xiamen University, Xiamen, Fujian 361005, People's Republic of China

Received May 5, 2006; E-mail: yirong.mo@wmich.edu

Abstract: Molecular dynamics (MD) simulations have been performed at the atomic level to study the ammonium/ammonia transport across the *Escherichia coli* AmtB membrane protein. Although ammonia primarily exists in the form of NH_4^+ in aqueous solution, the recent X-ray structure determination of AmtB reveals that the ammonium/ammonia transporter proteins are ammonia-conducting channels rather than ammonium ion transporters [Khademi, S.; et al. *Science* **2004**, *305*, 1587; Zheng, L.; et al. *Proc. Natl. Acad. Sci. U.S.A.* **2004**, *101*, 17090]. Our simulations showed that the entrance of NH_4^+ into the periplasmic recruitment vestibule requires only 3.1 kcal/mol of energy. This is consistent with the X-ray crystal structure, where one NH_4^+ is captured in the binding vestibule. In this vestibule, NH_4^+ loses one water of hydration, but the loss is compensated by a hydrogen bond, first with the backbone carbonyl oxygen of Phe161 then with the hydroxyl group of Ser219, as well as the stabilizing π-cation interactions with the aromatic rings of Trp148 and Phe107 in the AmtB protein. In the end of this recruitment vestibule, the phenyl ring of Phe107 dynamically switches to an open state. This is correlated with a slight rotation and shifting of the indole ring of Trp148, which eventually creates a slot for the initially buried carboxylate group of Asp160 to become exposed to the bulk solvent. A hydrogen bond wire between NH_4^+ and the carboxylate group of Asp160 via two water molecules was observed. Thus, Asp160 is most likely the proton acceptor from NH_4^+. This explains the high conservation of Asp160 in Amt proteins and why the D160A mutant would completely quench the activity of AmtB [Javelle, A.; et al. *J. Biol. Chem.* **2004**, *279*, 8530; Marini, A. M.; et al. *Curr. Genet.* **2006**, *49*, 364]. Once NH_4^+ deprotonates, the phenyl ring of Phe215 rotates to open, and the subsequent passage of NH_3 through the channel is straightforward.

Introduction

The Amt (ammonium transporter),[1] Mep (methylammonium permease),[2,3] and Rh (Rhesus)[4,5] membrane proteins form a superfamily which is ubiquitous in all domains of life and responsible for the transmembrane transport of ammonium/ammonia which is involved in the fundamental nitrogen metabolism.[6] Therefore, the transport of ammonia across cellular membranes is of high biological relevance. For example, for bacteria and plants, ammonia is an important nutrient that is taken from surroundings, such as air, to provide a source of nitrogen for amino acid synthesis, whereas for humans, ammonia is toxic at high concentration and mostly produced in renal cells from amino acids (mainly glutamine) and plays a critical role in the maintenance of our body's acid−base balance (pH regulation) through the regulation of renal ammonia excretion.[7] However, ammonia can exist in two forms in aqueous solution, namely, neutral NH_3 and positively charged ion NH_4^+, with the equilibrium constant (pK_a) for the following conversion being 9.25

$$NH_4^+ \rightleftharpoons NH_3 + H^+$$

Thus, at ambient condition and the ionic strength of blood plasma, the form of NH_4^+ is predominant. In principle, ammonium transduction across cell membranes can occur by direct NH_4^+ transport or by a combination of H^+ and NH_3 transport.[7] Passive NH_4^+ transport can be driven by a concentration gradient or an electrical potential gradient, whereas NH_3

[†] Western Michigan University.
[‡] Xiamen University.

(1) Jayakumar, A.; Hwang, S. J.; Fabiny, J. M.; Chinault, A. C.; Barnes, E. M. J. *J. Bacteriol.* **1989**, *171*, 996−1001.
(2) (a) Marini, A. M.; Vissers, S.; Urrestarazu, A.; Andre, B. *EMBO J.* **1994**, *13*, 3456−3463. (b) Ninnemann, O.; Jauniaux, J. C.; Frommer, W. B. *EMBO J.* **1994**, *13*, 3464−3471.
(3) von Wirén, N.; Gazzarrini, S.; Gojon, A.; Frommer, W. B. *Curr. Opin. Plant Biol.* **2000**, *3*, 254−261.
(4) (a) Marini, A. M.; Matassi, G.; Raynal, V.; Andre, B.; Cartron, J. P.; Chérif-Zahar, B. *Nat. Genet.* **2000**, *26*, 341−344. (b) Huang, C. H.; Peng, J. B. *Proc. Natl. Acad. Sci. U.S.A.* **2005**, *102*, 15512−15517. (c) Le Van Kim, C.; Colin, Y.; Cartron, J. P. *Blood Rev.* **2006**, *20*, 93−110.
(5) Westhoff, C. M.; Ferreri-Jacobia, M.; Mak, D. O. D.; Foskett, J. K. *J. Biol. Chem.* **2002**, *277*, 12499−12502.
(6) von Wirén, N.; Merrick, M. *Trends Curr. Genet.* **2004**, *9*, 95−120.
(7) Knepper, M. A.; Packer, R.; Good, D. W. *Physiol. Rev.* **1989**, *69*, 179−249.

10.1021/ja0631549 CCC: $33.50 **© 2006 American Chemical Society**

is moderately lipid soluble and is thought to penetrate cell membrane mainly by diffusion. At high concentration of ammonia/ammonium, passive membrane permeation of neutral NH_3 may be effective enough. At low concentration, however, a transport system is needed. This transport system is called ammonia/ammonium channels which exist in the Amt/Mep/Rh family membrane proteins. Up to now, over 200 genes belonging to this Amt/Mep/Rh family have been discovered.

Escherichia coli AmtB is an archetypal member of the Amt family and contains 406 amino acids which construct 11 transmembrane α-helices with a N-terminal periplasmic extension and a C-terminal cytoplasmic extension. In the native cytoplasmic membrane, AmtB forms a trimeric structure.[8] The transport rate is estimated to be $10-10^4$ ammonium molecules per second per channel, compared with the diffusion limit of 10^8-10^9 in an open channel.[9] Recently, the X-ray crystallographic structure of AmtB was resolved, and the structures complexed with ammonia or methylamine show that AmtB does act as a channel.[9,10] The most recent structure of Amt-1 from *Archaeoglobus fulgidus* further confirmed the above finding.[11] A similar concept of channel has been proposed for Rh proteins.[12,13] The X-ray structures reveal a recruitment vestibule for NH_4^+ which involves Phe103, Phe107, Trp148, and Phe215. These amino acids contain aromatic rings and can bind NH_4^+ via strong π-cation interactions. These π-cation interactions, which are arguably the strongest noncovalent interactions, are known to play a key role in numerous biological recognition processes, and the regulation of enzymatic activity and has been extensively studied.[14] The crystal structures also show that the phenyl rings of Phe107 and Phe215 serve as the gates for the ammonium/ammonia-conducting channel, which is highly hydrophobic and located at the center of each monomer of the trimeric AmtB. Thus, it is of general interest to explore the mechanism of gate opening, which is a dynamic process and hard to capture experimentally. Since there is no significant conformational change between AmtB structures with or without ammonium,[9,10] it must be the side chains that control the gate movement and the subsequent ammonia transport.

In terms of the exact form of transported species through ammonium/ammonia channels whose length is around 20 Å,[10] despite numerous studies, there have been uncertainties and speculations over whether a neutral ammonia (NH_3)[12,15−17] or positively charged ammonium (NH_4^+)[18−21] is more probable. In other words, whether the Amt/Mep/Rh proteins are involved in gas transport or ion transport has been debated. Unfortunately, although it is known that ammonia exists predominantly in a form of ammonium ion in biological fluids, it is difficult to measure ammonium directly, and its transport behavior can only be inferred from its inhibitory effect on methylamine uptake[18,19] or the measurement of ion current in oocytes.[5,17,20] It has been found that the accumulation of methylammonium (with ^{14}C label in experiments) in whole cells depends on Amt/Mep proteins, and thus it was inferred that Amt/Mep proteins mediate the uptake of ammonium ions.[3] However, accumulating evidence shows that Amt/Mep proteins can increase the rate of equilibrium of ammonia across the cytoplasmic membrane and thus are channels for ammonia.[15] Evidently, the recent X-ray structure of AmtB clarified that NH_3 is indeed the species conducted through the channel.[9,10] This is further endorsed by in vivo data which show that AmtB function is independent of either the membrane potential or the intracellular ATP pool.[22]

As the conducted species has now been confirmed to be ammonia, the subsequent question is where and how the initial ammonium deprotonates. No direct experimental evidence is available in this regard. As a matter of fact, few experiments toward the elucidation of the deprotonation mechanism have ever been done since the ammonia channels were widely believed to be ion rather than gas channels. Notably, there are two highly conserved residues in the mid-membrane center of the pathway, His168 and His318, which are hydrogen bonded with each other and unprotonated. There are speculations that these histidines may serve as proton acceptors for ammonium ions.[9] However, the subsequent diffusion of protons from these histidines back to the periplasmic phase seems problematic as there is no apparent proton transfer route from the inner channel to the external solution with the gates (Phe107 and Phe213) closed.

Whereas crystallographic structures provide clear yet static pictures of the three-dimensional spatial arrangement of atoms, little knowledge is available about the transient conformations in the biological processes (for example, enzyme-catalyzed reactions and transportation of ions or molecules). However, recent evidence shows that dynamics plays a critical role in the functions of proteins.[23] Computational studies have the potential to correlate the structures, dynamics, and functions of proteins, thus they are able to complement experimental information.[24] Molecular dynamics (MD) simulations of membrane proteins

(8) (a) Blakey, D.; Leech, A.; Thomas, G. H.; Coutts, G.; Findlay, K.; Merrick, M. *Biochem. J.* **2002**, *364*, 527−535. (b) Conroy, M. J.; Jamieson, S. J.; Blakey, D.; Kaufmann, T.; Engel, A.; Fotiadis, D.; Merrick, M.; Bullough, P. A. *Embo Rep.* **2004**, *5*, 1153−1158.
(9) Zheng, L.; Kostrewa, D.; Berneche, S.; Winkler, F. K.; Li, X. D. *Proc. Natl. Acad. Sci. U.S.A.* **2004**, *101*, 17090−17095.
(10) Khademi, S.; O'Connell, J.; Remis, J.; Robles-Colmenares, Y.; Miericke, L. J. W.; Stroud, R. M. *Science* **2004**, *305*, 1587−1594.
(11) Andrade, S. L. A.; Dickmanns, A.; Ficner, R.; Einsle, O. *Proc. Natl. Acad. Sci. U.S.A.* **2005**, *102*, 14994−14999.
(12) Ripoche, P.; Bertrand, O.; Gane, P.; Birkenmeier, C.; Colin, Y.; Cartron, J. P. *Proc. Natl. Acad. Sci. U.S.A.* **2004**, *101*, 17222−17227.
(13) Conroy, M. J.; Bullough, P. A.; Merrick, M.; Avent, N. D. *Brit. J. Haematol.* **2005**, *131*, 543−551.
(14) (a) Dougherty, D. A.; Stauffer, D. A. *Science* **1990**, *250*, 1558−1560. (b) Burley, S. K.; Petsko, G. A. *FEBS Lett.* **1986**, *203*, 139−143. (c) Scrutton, N. S.; Raine, A. R. C. *Biochem. J.* **1996**, *319*, 1−8. (d) Ma, J. C.; Dougherty, D. A. *Chem. Rev.* **1997**, *97*, 1303−1324. (e) Gallivan, J. P.; Dougherty, D. A. *Proc. Natl. Acad. Sci. U.S.A.* **1999**, *96*, 9459−9464. (f) Mo, Y.; Subramanian, G.; Gao, J.; Ferguson, D. M. *J. Am. Chem. Soc.* **2002**, *124*, 4832−4837. (g) Liu, Y. M.; Hu, X. H. *J. Phys. Chem. A* **2006**, *110*, 1375−1381.
(15) (a) Soupene, E.; Ramirez, R. M.; Kustu, S. *Mol. Cell Biol.* **2001**, *21*, 5733−5741. (b) Soupene, E.; Lee, H.; Kustu, S. *Proc. Natl. Acad. Sci. U.S.A.* **2002**, *99*, 3926−3931.
(16) Meier-Wagner, J.; Nolden, L.; Jakoby, M.; Siewe, R.; Kramer, R.; Burkovski, A. *Microbiol.* **2001**, *147*, 135−143.
(17) Bakouh, N.; Benjelloun, F.; Hulin, P.; Brouillard, F.; Edelman, A.; Cherif-Zahar, B.; Planelles, G. *J. Biol. Chem.* **2004**, *279*, 15975−15983.
(18) Kleiner, D. *FEMS Microbiol. Rev.* **1985**, *32*, 87−100.
(19) Marini, A. M.; Soussi-Boudekou, S.; Vissers, S.; Andre, B. *Mol. Cell Biol.* **1997**, *17*, 4282−4293.
(20) Ludewig, U.; von Wirén, N.; Frommer, W. B. *J. Biol. Chem.* **2002**, *277*, 13548−13555.
(21) (a) Ludewig, U. *J. Physiol.* **2004**, *559*, 751−759. (b) Nakhoul, N. L.; Dejong, H.; Abdulnour-Nakhoul, S. M.; Boulpaep, E. L.; Hering-Smith, K.; Hamm, L. L. *Am. J. Physiol. Renal. Physiol.* **2005**, *288*, F170−F181.
(22) Javelle, A.; Thomas, G.; Marini, A. M.; Kramer, R.; Merrick, M. *Biochem. J.* **2005**, *390*, 215−222.
(23) (a) Eisenmesser, E. Z.; Bosco, D. A.; Akke, M.; Kern, D. *Science* **2002**, *295*, 1520−1523. (b) Eisenmesser, E. Z.; Millet, O.; Labeikovsky, W.; Korzhnev, D. M.; Wolf-Watz, M.; Bosco, D. A.; Skalicky, J. J.; Kay, L. E.; Kern, D. *Nature* **2005**, *438*, 117−121. (c) Masgrau, L.; Roujeinikova, A.; Johannissen, L. O.; Hothi, P.; Basran, P.; Ranaghan, K. E.; Mulholland, A. J.; Sutcliffe, M. J.; Scrutton, N. S.; Leys, D. *Science* **2006**, *312*, 237−241.
(24) (a) Benkovic, S. J.; Hammes-Schiffer, S. *Science* **2003**, *301*, 1196−1202. (b) Garcia-Viloca, M.; Gao, J.; Karplus, M.; Truhlar, D. G. *Science* **2004**, *303*, 186−195. (c) Agarwal, P. K. *J. Am. Chem. Soc.* **2005**, *127*, 15248−15256.

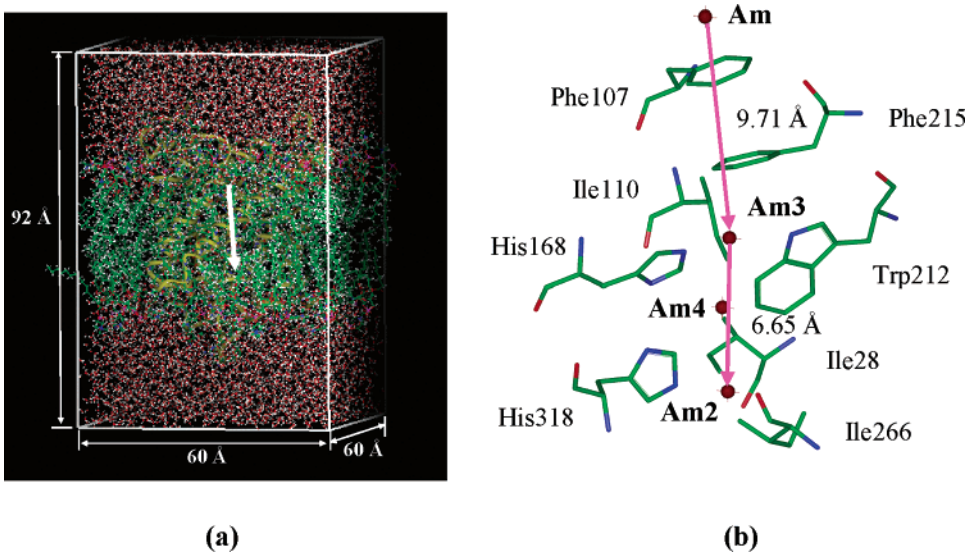

Figure 1. (a) Final AmtB membrane protein model (unitary cell) for simulations, where the white arrow highlights the ammonia channel and the ribbon structure is shown in yellow. Atom colors are red for oxygen, blue for nitrogen, green for carbon, and white for hydrogen. (b) The ammonia-conducting channel in AmtB with one ammonium (Am) outside the channel and three ammonia molecules (Am2, Am3, and Am4) inside the channel in the crystallographic structure.[10]

at the atomic level can reveal the dynamic behavior of membrane proteins in the biological processes and provide insights into the physical mechanisms and the physical principles underlying these processes.[25] Membrane proteins which have been computationally simulated include ion channels (of particular potassium, calcium, and chloride channels), aquaporins, and bacteriorhodopsin. To probe the transport mechanism, we simulated the transduction of ammonium/ammonia through the membrane protein AmtB in silico. In particular, free energy profiles were derived based on the umbrella sampling technique. Our MD simulations were intended to address the following mechanistic questions: (1) the recruitment of ammonium ions from the bulk solution to the periplasmic binding vestibule; (2) the gating mechanism of the channel, where the gates are the phenyl rings of Phe107 and Phe215; (3) the ammonium deprotonation mechanism; (4) the energy profile for the passage of ammonia through the channel; and (5) the selectivity of the channel toward water molecules and whether water can pass the channel, either alone or following ammonia in a water−ammonia pair as there is weak hydrogen bonding interaction between them.

Methods

Computational Model. AmtB forms a trimeric structure in the native cytoplasmic membrane,[8] and the channels are located in the middle of monomers, which are bound together by hydrophobic forces. Thus, these channels must function individually. To reduce the computational costs, we use a monomeric form of AmtB to run simulations. Our subsequent MD simulations confirm the feasibility of this monomeric model as the RMS deviation of the monomer with reference to the crystal structure ranges from 1.45 to 1.60 Å, close to the resolution (1.35 Å) of the crystal structure.[10] The complete computational model is built based on the established procedure detailed by Woolf and Roux.[26] The AmtB monomer is embedded in a phospholipid bilayer constructed with DMPC (1,2-dimyristoyl-*sn*-glycero-3-phosphocholine) to imitate the membrane environment. The X-ray structure of AmtB at an atomic resolution of 1.35 Å determined by Khademi et al. was used in this work (Protein Data Bank ID code 1U7G).[10] The three mutated residues (F68S, S126P, and K255L) and engineered Met residues (S atoms were replaced by Se) in 1U7G were modified back to their native states. Hydrogen positions of the protein are incorporated using the HBUILD facility in CHARMM[27] based on heavy atom positions and standard bond lengths and angles. The protonated states of histidine residues are determined based on their individual microenvironments; for instance, both His168 and His318 are found to be neutral, but the proton is attached to ND1 in the imidazole ring for His168, whereas the proton is on NE2 for His318. Water slabs of 30 Å thick are subsequently added to both the top and bottom of the phospholipid bilayer. The final model (Figure 1a), in the size of 60 × 60 × 92 Å^3, consists of about 35 000 atoms, including the AmtB protein, 72 DMPC molecules, 6414 water molecules, as well 2−3 chloride ions to neutralize the whole system. This model is further extended with periodic boundary condition (PBC). The electrostatic interactions are computed with no truncation using the particle mesh Ewald (PME) algorithm.[28] The trajectories are generated with a time step of 1 fs at constant pressure and temperature (300 K).

Coordinate for Energy Profiles. In terms of reaction coordinate for the free energy simulations, we chose a site around the end of the channel as the reference point. Apart from an ammonium ion (Am) in the recruitment vestibule, Khademi et al. observed three weak electron density peaks within the hydrophobic channel which were interpreted to be partially occupied ammonia molecules (Am2, Am3, and Am4 in Figure 1b).[10] Interestingly, these four ammonium/ammonia sites are nearly in line. Accordingly, we take the position of Am2, which is in the downside of the channel, as the origin of the coordinate to describe the movement of ammonium/ammonia and plot the corresponding

(25) (a) Bernèche, S.; Roux, B. *Nature* **2001**, *414*, 73−77. (b) de Groot, B. L.; Grubmüller, H. *Science* **2001**, *294*, 2353−2357. (c) Tajkhorshid, E.; Nollert, P.; Jensen, M. Ø.; Miercke, L. J. W.; O'Connell, J.; Stroud, R. M.; Schulten, K. *Science* **2002**, *296*, 525−530. (d) Hansson, T.; Oostenbrink, C.; van Gunsteren, W. F. *Curr. Opin. Struct. Biol.* **2002**, *12*, 190−196. (e) Lehnert, U.; Xia, Y.; Royce, T. E.; Goh, C.-S.; Liu, Y.; Senes, A.; Yu, H.; Zhang, Z. L.; Engelman, D. M.; Gerstein, M. *Q. Rev. Biophys.* **2004**, *37*, 121−146. (f) Roux, B.; Allen, T.; Bernèche, S.; Im, W. *Q. Rev. Biophys.* **2004**, *37*, 15−103. (g) Gumbart, J.; Wang, Y.; Aksimentiev, A.; Tajkhorshid, E.; Schulten, K. *Curr. Opin. Struct. Biol.* **2005**, *15*, 423−431. (h) Karplus, M.; Kuriyan, J. *Proc. Natl. Acad. Sci. U.S.A.* **2005**, *102*, 6679−6685.

(26) (a) Pastor, R. W.; Venable, R. M.; Karplus, M. *Proc. Natl. Acad. Sci. U.S.A.* **1991**, *88*, 892−896. (b) Venable, R. M.; Zhang, Y. H.; Hardy, B. J.; Pastor, R. W. *Science* **1993**, *262*, 223−226. (c) Woolf, T. B.; Roux, B. *Proc. Natl. Acad. Sci. U.S.A.* **1994**, *91*, 11631−11635.

(27) Brooks, B. R.; Bruccoleri, R. E.; Olafson, B. D.; States, D. J.; Swaminathan, S.; Karplus, M. *J. Comput. Chem.* **1983**, *4*, 187−217.

(28) Essmann, U.; Perera, L.; Berkowitz, M. L.; Darden, T.; Lee, H.; Pedersen, L. G. *J. Chem. Phys.* **1995**, *103*, 8577−8593.

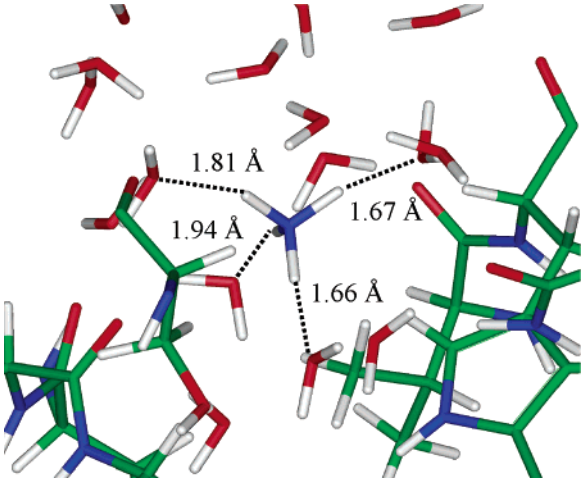

Figure 2. A snapshot for the initial configuration of an ammonium ion outside the AmtB membrane protein, where the ion is fully solvated (R_c = −20.2 Å).

energy profiles. It should be noted, however, that the pathways of ammonium/ammonia are not constrained to be linear at all in MD simulations.

Computational Details. All simulations were carried out with CHARMM.[27] The all-atom empirical potential energy function for proteins[29] and phospholipids[30] was used. For the water molecules, the TIP3P potential was used.[31] Mulliken charges at the HF/6-31G(d) were employed for nitrogen and hydrogen atoms in ammonium/ammonia, whose Lennard-Jones (LJ) parameters were kept the same as those for amide groups. The list of nonbonded interactions was truncated at 13 Å, and the van der Waals and electrostatic interactions were smoothly switched off in the range of 11−12 Å. Umbrella sampling technique was adopted to generate the free energy profile or potential of mean force (PMF) along the transduction trajectory. A biasing harmonic potential with a force constant of 15−20 kcal/mol was imposed in simulations which were separated by 0.4 Å, that is, there would be 50 independent simulations for the transport of ammonium/ammonia of 20 Å distance. Overall, the trajectory of the ammonium transport was simulated with 40 windows, and either of the two trajectories of the ammonia transport was projected out with 75 simulations. For each window, the first 50 ps simulation brought the system to an equilibrium state, and the second 50 ps simulation generated dynamics data for further analyses. In the simulations, all of the bonds with hydrogen atoms in AmtB will be constrained with the SHAKE algorithm.[32]

Results and Discussion

Recruitment of NH_4^+ to the Binding Vestibule. To fully understand the whole process of the ammonium/ammonia transport across AmtB, we started with a state where the ammonium ion is completely solvated by aqueous solution and has no direct interactions with the membrane protein. We chose a site which is outside the protein and has a distance of around 20.7 Å with the reference point for NH_4^+. A few umbrella sampling simulations separated by 0.4 Å were performed around this site. Slight energetic fluctuation (±0.7 kcal/mol) is observed, and a minimum is located at a distance of about 20 Å. A snapshot at this site is shown in Figure 2, where a solvent shell

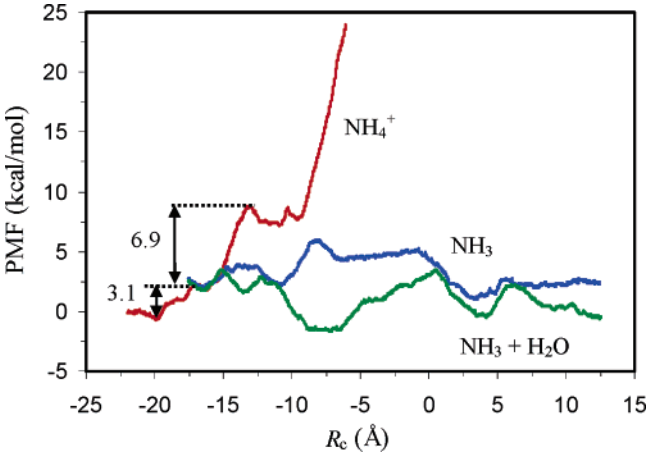

Figure 3. Potential of mean force (PMF) profiles for the passage of ammonium/ammonia across the AmtB membrane protein. The free energy at the starting configuration is referenced as zero. The energy change along the transduction of NH_4^+ is plotted in red. As NH_4^+ most probably deprotonates in the end of the periplasmic recruitment vestibule (−16 Å), the free energy profiles for the transduction of NH_3 alone (in blue) or coupled with one water (in green) are made to overlap with the curve of NH_4^+ at this position.

composed of about four water molecules forms hydrogen bonds with the ammonium ion and the slight stabilization may result from the indirect interaction with the protein environment (i.e., long-range electrostatic interactions). As the solvation free energy of the ammonium ion in water is around 80 kcal/mol,[33] NH_4^+ reaches its energy minimum at this state. Starting from this configuration, more umbrella sampling simulations were conducted to slowly move the ion toward and through the channel gates. Figure 3 plots the free energy profile along the transport of NH_4^+ from bulk solvent to the binding vestibules and into the channel (curve in red). Once NH_4^+ begins to interact with the protein residues directly, two binding regions for the ion, in the ranges of −17.1 to −15.5 Å and −12.2 to −9.2 Å, were identified. We note that the first binding region (recruitment vestibule) is consistent with the X-ray crystal structure where an ammonium ion is captured (Am in Figure 1b, R_c = −16.3 Å). The first binding region is located in the outside of the channel, and the second one is inside the channel.

Javelle et al.[22] examined the temperature dependence of methylammonium uptake by AmtB from 4 to 37 °C and determined an activation energy (E_a) of 1.6 kcal/mol, which confirms that AmtB functions as a channel rather than a transporter. For comparison, the E_a of transporters usually ranges from 11 to 27 kcal/mol.[34] Our energy profile (red curve in Figure 3) shows that the first binding site for NH_4^+ requires only 3.1 kcal/mol of energy, in good agreement with the experimental measurement. Figure 4a presents a snapshot (at R_c = −17.8 Å) just before NH_4^+ climbs into the first ion-binding vestibule. At this snapshot, NH_4^+ loses one water molecule in its first hydration shell, but the energetic loss is mostly compensated by the hydrogen bond with the backbone carbonyl oxygen of Ala162 (when NH_4^+ floats away a little bit, it can also bind to the backbone carbonyl oxygen of Phe161) as well as the π-cation interaction with Trp148. As a consequence, the overall solvation energy reduction is trivial. With the further movement

(29) MacKerell, A. D.; et al. *J. Phys. Chem. B* **1998**, *102*, 3586−3616.
(30) Schlenkrich, M.; Brickmann, J.; MacKerell, A. D., Jr.; Karplus, M. In *Biological Membranes: A Molecular Perspective from Computation and Experiment*; Merz, K. M., Jr., Roux, B., Eds.; Birkhäuser: Boston, 1996; pp 31−81.
(31) Jorgensen, W. L.; Chandrasekhar, J.; Madura, J. D.; Impey, R. W.; Klein, M. L. *J. Chem. Phys.* **1983**, *79*, 926−935.
(32) van Gunsteren, W. F.; Berendsen, H. J. C. *Mol. Phys.* **1977**, *34*, 1311−1327.
(33) (a) Pearson, R. G. *J. Am. Chem. Soc.* **1986**, *108*, 6109−6114. (b) Cao, Z.; Lin, M.; Zhang, Q.; Mo, Y. *J. Phys. Chem. A* **2004**, *108*, 4277−4282.
(34) Liu, G.; Hinch, B.; Davatol-Hag, H.; Lu, Y.; Powers, M.; Beavis, A. D. *J. Biol. Chem.* **1996**, *271*, 19717−19723.

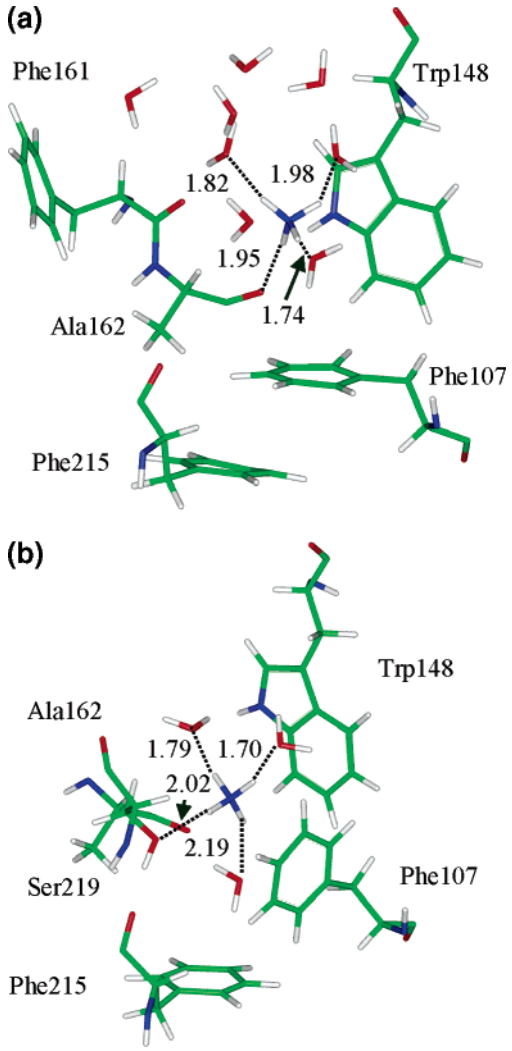

Figure 4. Snapshots illustrating the surroundings for the ammonium ion in the first binding region: (a) just before reaching the first binding site ($R_c = -17.8$ Å); (b) in the periplasmic recruitment ($R_c = -16.4$ Å).

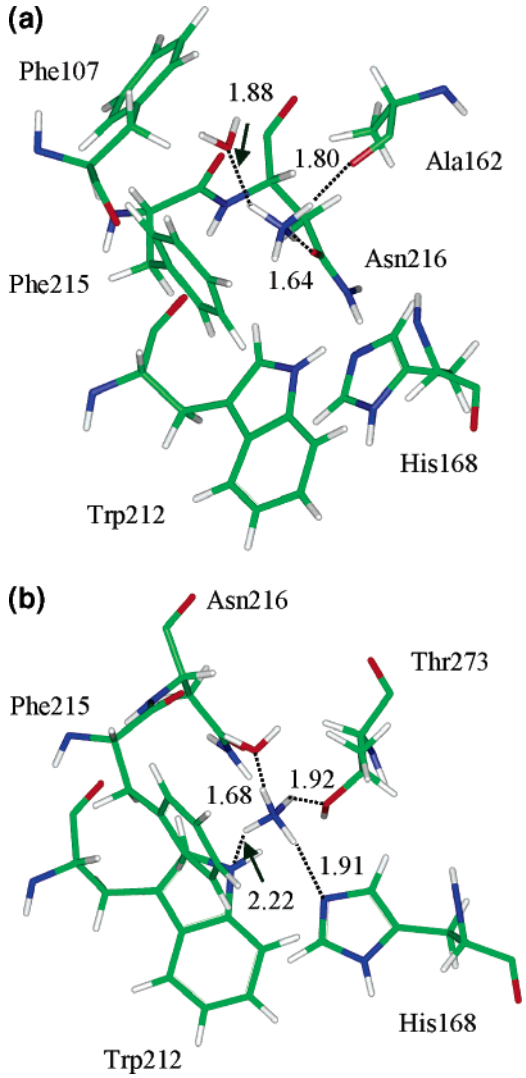

Figure 5. Snapshots illustrating the surroundings for the ammonium ion in the second binding region: (a) in the first part of the second binding region ($R_c = -11.8$ Å); (b) in the second part of the second binding region ($R_c = -9.7$ Å).

of NH_4^+ toward the channel, NH_4^+ falls into the binding vestibule, which is composed of Phe107, Trp148, Phe215, and Ser219. Ser219 plays its role by forming a strong hydrogen bond with NH_4^+, whereas the aromatic rings of both Trp148 and Phe107 bind NH_4^+ via π-cation interactions. As a result, in the range from -17 to -16 Å, the free energy changes little. The interesting finding in this range is that the first gate of the channel (the phenyl ring of Phe107) starts to open dynamically. Figure 4b shows a snapshot at $R_c = -16.4$ Å, where the phenyl ring of Phe107 has rotated nearly 90° to be perpendicular to the aromatic ring of Phe215, which still blocks the channel (more discussion in this regard can be found in the following subsection). When NH_4^+ enters into the narrow, mostly hydrophobic (with the exception of Ser219) recruitment vestibule, we found that one water molecule can also fall into the vestibule and directs its hydrogen to the aromatic ring of Phe215 (see Figure 4b). Thus, it is of interest to examine the possible fate of this water molecule.

The second binding site (-12.2 to -9.2 Å) is located in the beginning of the channel, and NH_4^+ has already entered into the channel. One water molecule is observed to follow NH_4^+ into the channel due to the strong hydrogen bonding interaction between them. While Phe107 has already returned to its original position and closed the channel, Phe215 starts to open its gate as its phenyl ring, together with Trp212, forms a binding pocket for NH_4^+ via stabilizing π-cation interactions. Apart from one hydrogen bond with water, the ion forms hydrogen bonds with surrounding residues. Interestingly, we also observed a noticeable barrier (1.3 kcal/mol) in the middle of the second binding region, which is thus divided into two areas of similar energies. Two representative snapshots for these two areas are shown in Figure 5. In both cases, the ammonium ion interacts with the aromatic ring of Phe215 noticeably. In the first area (Figure 5a, where $R_c = -11.8$ Å), except for one hydrogen pointing toward the phenyl ring of Phe215, the rest of the three hydrogens in NH_4^+ form hydrogen bonds with water, the backbone carbonyl oxygen at Ala162, and the carbonyl oxygen at Asn216. In the second area (Figure 5b, where $R_c = -9.7$ Å), however, there is a significant change for the binding mode of NH_4^+, which now binds His168, Thr273, and Trp212. The small barrier between these two areas thus reflects the shifting of hydrogen bonds.

Compared with the first binding region (Figure 4b), there is a considerable energy loss for the system at the second binding

region by 5.6 kcal/mol, and the barrier between these two sites is about 6.9 kcal/mol (Figure 3). This is somewhat lower than the estimated electrostatic barrier of 10 kcal/mol determined by Zheng et al.,[9] who also suggested that NH_4^+ may lose its proton at this site to His168. Energetically, it seems probable, although it is certainly more favorable for NH_4^+ to deprotonate at the first binding site as the barrier from the first to the second binding site is about 6.9 kcal/mol. However, one concern for this deprotonation mechanism at the second binding site is how the proton can be shipped out of this channel. Also, we note there is no water found in the crystal structure, suggesting no appropriate hydrogen bond chain via water molecules to facilitate the transduction of a proton out of the channel. Besides, the protonated His168 is still around NH_3, and there will be a strong electrostatic attraction between them. Moving NH_3 down the channel thus will be energetically very costly.

After the second binding site, a sharp increase of energy is observed if the ammonium ion keeps moving down the hydrophobic channel, largely due to the high desolvation cost and the lack of effective hydrogen bonds with the channel. This strongly confirms that ammonium ions cannot go through the very hydrophobic channel, and the conducted species thus must be neutral ammonia molecules.

Gating Mechanism. Crystal structures of AmtB reveal two gates, namely, the phenyl rings of Phe107 and Phe215, in the entrance of the channel (Figure 1b). In both structures with and without ammonia or methylamine, these two gates are parallel and block the channel.[10] Thus, the passage of ammonium/ammonia through the gates must be a dynamic and fast process. However, when NH_4^+ is away from the binding vestibule, no significant movement of the two phenyl rings of Phe107 and Phe215 was found. With the approach of NH_4^+ to the first gate, we observed a rotation of the phenyl ring of Phe107 to facilitate the passage of the invader. Figure 6a illustrates this process by superimposing 12 snapshots along the movement of NH_4^+ in the range from −20.2 to −6.7 Å for R_c. Obviously, the gate opening is not a continuous process, rather, a dynamic process. More specifically, there are only two states for Phe107, namely, "closed" (perpendicular to the channel) or "open" (parallel to the channel). When NH_4^+ gets close to Phe107, the latter will choose the open state; otherwise, it will stay in the closed state. This gate-opening process does not require additional energy and thus is a very fast process which starts to appear in the first binding vestibule. We assume that a favorable orientation for the π-cation interaction between NH_4^+ and the aromatic ring of Phe107 may be the cause. Figure 4b also shows that, in the end of the first binding vestibule, the gate is already open.

The continuous transport of NH_4^+ gradually pushed the second gate, the phenyl ring of Phe215, open. However, this process accompanies a high energy cost as depicted by the free energy profile in Figure 3, although this energy cost may be mainly due to the loss of hydrogen bonds with water molecules which are shut out of the channel due to the narrowness and hydrophobicity of the channel. When NH_4^+ falls into the second binding region, the first gate is still open, but once NH_4^+ leaves the first gate far enough and binds to His168, the first gate returns to the closed state. Thus, we conclude that NH_4^+ is responsible for the opening of the first gate of Phe107 but not the second gate of Phe213. Instead, we found a deprotonation mechanism (see the following subsection) for NH_4^+ in the first binding vestibule, and the subsequent neutral ammonia will open the second gate dynamically and effectively (Figure 6b).

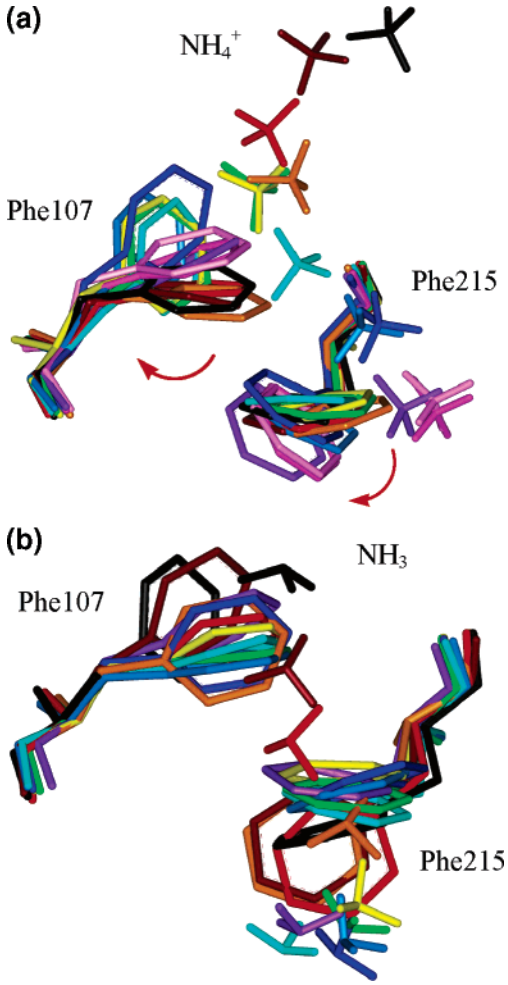

Figure 6. The dynamic opening of the gates by (a) the ammonium ion (superimposed snapshots at R_c = −20.2, −19.3, −17.8, −16.8, −16.3, −14.5, −13.2, −12.0, −10.9, −9.6, −8.1, and −6.7 Å in color from black to magenta); (b) the ammonia (superimposed snapshots at R_c = −15.6, −14.1, −13.0, −11.3, −9.9, −8.7, −8.0, −7.4, −6.5, and −5.7 Å in color from black to purple).

Role of Asp160 and Deprotonation Mechanism of NH_4^+. There are two highly conserved aspartate residues, Asp160 and Asp310, in the Amt proteins of bacteria, fungi, and plants. Whereas there is no evidence yet to show that they actively participate in the ammonia transporting process, their roles are generally believed to be structural as their acidic side chains form hydrogen bonds with main chain N−H groups (residues 163−165 and 314−316, respectively). These hydrogen bonding interactions can fix the backbone of the helical structure preceding His168 and His318,[9] although structural modeling of the AmtB protein suggested Asp160 as a potential candidate for an initial ammonium binding site on the periplasmic face of the membrane.[35] Mutation of Asp160 to Ala160, nevertheless, completely disables the transporting capability, while the D160E mutant retains 71% of the activity of the wild type.[36] Furthermore, X-ray structures clearly rule out the possibility for Asp160 as a binding site for the ammonium ion. It has been shown that Asp160 is a helix-capping residue for the fifth helix of AmtB and its carboxylate group forms hydrogen bonds with Thr165, Gly164, and Gly163 at the N-terminal end of the fifth helix.

(35) Thomas, G. H.; Mullins, J. G.; Merrick, M. *Mol. Microbiol.* **2000**, *37*, 331−344.
(36) Javelle, A.; Severi, E.; Thornton, J.; Merrick, M. *J. Biol. Chem.* **2004**, *279*, 8530−8538.

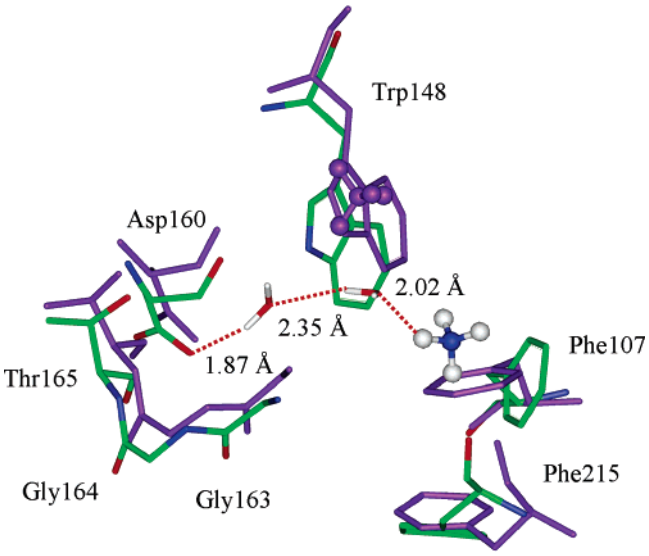

Figure 7. The superimposition of two snapshots, where NH_4^+ is in the bulk solvent ($R_c = -20.2$ Å, in purple) and in the first binding region ($R_c = -15.8$ Å, in multicolors). The hydrogen bond chain between Asp160 and NH_4^+ mediated by water molecules is highlighted by the dashed red line.

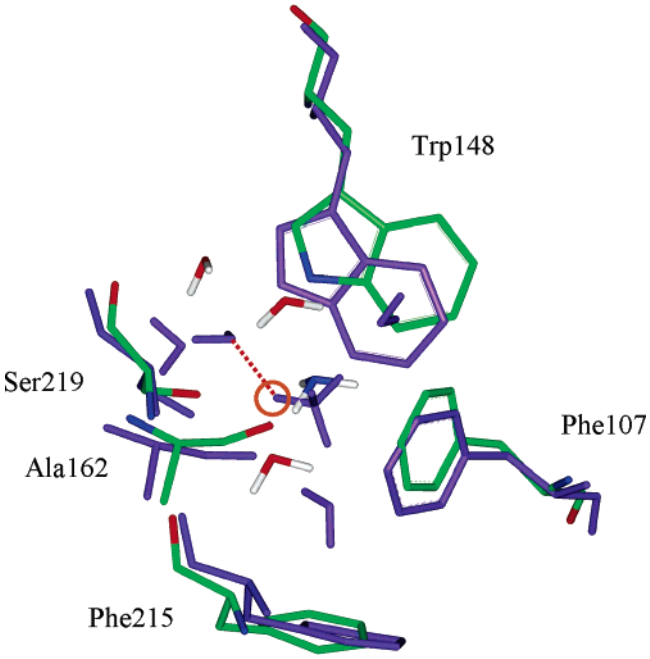

Figure 8. Snapshots before (in purple) and after (in multicolor) the deprotonation of ammonium ion at the binding vestibule ($R_c = -15.8$ Å). The transferred proton is highlighted with a circle in orange.

Although it is an ionic residue, Asp160 itself is not accessible to any solvent molecule since the indole ring of Trp148 is interposed between Asp160 and the binding vestibule for NH_4^+ and thus shields Asp160 from solvent.[10] One of the major conclusions from the analysis of static crystallographic structures is that the role of Asp160 is primarily structural. Most recently, Marini et al. also confirmed the critical role of an analogous aspartate residue for the transport function of eukaryotic family members as distant as the yeast transporter/sensor Mep2 and the human RhAG and RhCG proteins.[37]

Of significant interest, we found that, in the periplasmic binding vestibule, the dynamic flipping of the phenyl ring of Phe107 is accompanied by a slight rotation and shifting of the indole ring of Trp148. Meanwhile, the carboxylate group of Asp160 rotates and subsequently reorients the carbonyls (backbone) of Gly163 and Ala162. All these collective movements accumulate to a slot for Asp160 to become exposed to the bulk solvent, and one water molecule eventually manages to enter into the slot to bond with the carboxylate group. This water molecule connects to another solvent molecule which is in the first hydration shell of NH_4^+. As a consequence, we observed an ideal hydrogen bond wire between NH_4^+ and the carboxylate group CO_2^- of Asp160 through two water molecules. Figure 7 depicts the changes of the surroundings of the carboxylate group of Asp160 with the approach of an ammonium ion from bulk solvent to the first binding vestibule. Therefore, *Asp160 is most likely the proton acceptor from ammonium ions*. This explains the extreme importance of this residue and why the D160A mutant completely quenches the activity of AmtB. Marini et al. also stated that "the conserved aspartate residue likely plays a preserved functional role in Mep/Amt/Rh proteins" based on their experimental finding that the transport and sensing functions of this aspartate residue are not dissociated.[37]

However, at present, there is no direct experimental evidence to verify our computational findings regarding the specific functional role of Asp160. The lack of research in this aspect is mainly due to the fact that, only until very recently when the X-ray structures were accessible, the ammonia transporter proteins were thought to be ion channels. Due to the static nature of X-ray structures, however, the role of Asp160 is only recognized to be structural. To find the probable proton acceptor, other than Asp160, Zheng et al. proposed that His168, bridged with His318 via a H-bond, might facilitate the deprotonation of the ammonium ion[9] in the second binding site, but as we pointed out in the pretext, there are enough concerns not to pursue this hypothesis. In addition, our energetic analysis showed that the energy barrier to move NH_4^+ from the first binding site to the second binding site is 6.9 kcal/mol. Thus, we expect the deprotonation process occurs in the first binding site, particularly, with Asp160 as the proton acceptor.

Continuous Conduction of Neutral NH_3 in the Channel. As the deprotonation of ammonium ions most probably occurs in the periplasmic ion-binding vestibule and Asp160 is the proton acceptor mediated by two water molecules via a hydrogen bond wire, we proceeded to determine the free energy profile for the conduction of ammonia through the channel starting from this site. We chose an equilibrium configuration after 100 ps simulation for the ammonium ion and AmtB membrane model at $R_c = -15.8$ Å and removed the proton pointing toward the carboxylate group of Asp160. The subsequent 100 ps simulation for the ammonia and AmtB membrane protein model perturbs the amino acid orientations surrounding the neutral ammonia due to the dramatic reduction of hydrogen bonds of substrate (NH_3) with Ser219 and water molecules compared with the ammonium ion. Figure 8 superimposes two snapshots of NH_4^+ and NH_3 in the binding vestibule (at $R_c = -15.8$ Å). Consistent with the very low solvation energy of ammonia (4.3 kcal/mol[38]), in contrast to the very high value of ammonium ion (~80 kcal/mol[33]), the water molecules around NH_3 tend to move away, apparently due to the greatly weakened hydrogen bonds, and

(37) Marini, A. M.; Boeckstaens, M.; Benjelloun, F.; Chérif-Zahar, B.; Andre, B. *Curr. Genet.* **2006**, *49*, 364−374.

(38) Marten, B.; Kim, K.; Cortis, C.; Friesner, R. A.; Murphy, R. B.; Ringnalda, M. N.; Sitkoff, D.; Honig, B. *J. Phys. Chem.* **1996**, *100*, 11775−11788.

ammonia reorientates to make the nitrogen lone pair point toward the solvent side to form a hydrogen bond with solvent molecules. Notably, the water molecule just above the phenyl ring of Phe215 (also see Figure 4b) loses the binding to NH_3, but it is still trapped in the vestibule. Due to the hydrophobic nature of the deep site formed by Ala162, Phe215, and Phe107, it is difficult for water to reside stably in this pocket as the favorable water−water interactions can slightly stabilize the system. Thus, with the deprotonation of NH_4^+, the trapped water molecule has a tendency to move back the bulk solvent. However, our test simulations starting from this site but with different equilibrium conformations suggest that this trapped water may go through the channel coupled with the ammonia before being able to get out. As a consequence, we performed complete simulations on two trajectories, one with NH_3 alone and the other with the NH_3−H_2O complex, whose free energy profiles are plotted in Figure 2. Note that we do not impose any restraint on the NH_3−H_2O complex in the second case.

The passage of ammonia through the channel is relatively smooth, and the biggest bump is only 3.6 kcal/mol. When the ammonia travels alone, the first energy minimum is found at around −11.1 Å, due to the favorable hydrogen bond between NH_3 and His168. The energy maximum appears at −8.3 Å and may result from the environmental effect (i.e., the electrostatic field imposed by the surrounding protein environment) as we do not observe any immediate interactions except the hydrogen bond with His168. After a long movement with the breaking of the hydrogen bond with His168, NH_3 starts to stabilize slightly again at 3.8 Å by forming a hydrogen bond with His318. A further transduction without a noticeable barrier makes the ammonia exit the channel at $R_c = 8$ Å, where Phe31 holds the gate. However, we do not observe the rotation of the phenyl ring of Phe31. Instead, the ammonia gets out of the channel around the phenyl ring. Since the passage of ammonia through AmtB is a freely reversible process and a specific base (Asp160) is required for the deprotonation of the ammonium on the periplasmic side, there must also be a specific base for deprotonation on the cytosolic side for transport in the reverse (and an acid for the forward transport).[39] We examined the structure and found that, at the exit ($R_c = 9$ Å), the ammonia connects via two water molecules to the carboxylate group of Asp313 and the ammonium group of Lys303, which may play roles in the protonation/deprotonation of ammonia/ammonium on the cytosolic side (see Figure S1 in the Supporting Information).

The trajectory of the NH_3−H_2O complex is somewhat different due to the involvement of the water. For instance, the first minimum comes early at −13.5 Å due to the NH_3···H_2O···His168 hydrogen bridge. In contrast to the maximum state for the first trajectory at −8.3 Å, the $NH_3 + H_2O$ complex finds the minimum state at this site. Figure 9 compares the snapshots of the two trajectories at this region. Apart from the different orientations of the conducted species, there are no other apparent discrepancies. We therefore surmise the difference originates from the environment effect. Both energy profiles reach minima together at 3.8 Å as at this moment the water in the second case has already slipped out of the channel. In the simulations, we do not observe any other external water coming into the channel from either the top or the bottom. This is different from the simulations of the transduction of the ammonium ion, where we observe water molecules coming from the bottom due to the strong electrostatic attraction from the cation.

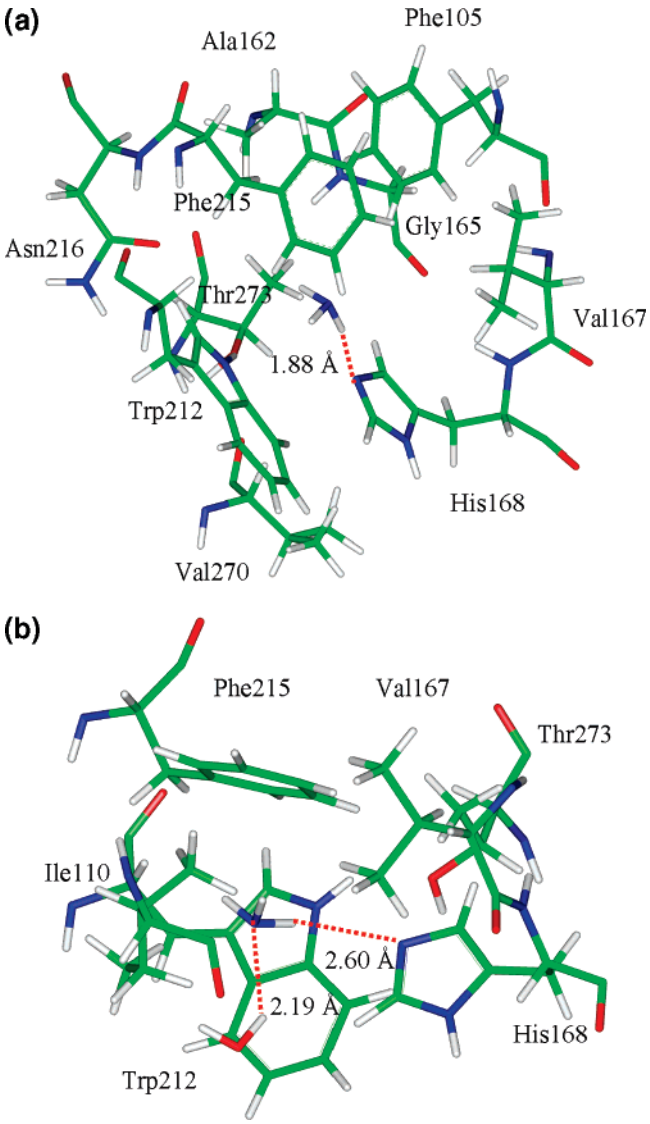

Figure 9. Snapshots of the passage of ammonia alone (a) or coupled with a water molecule (b) through the hydrophobic channel of AmtB ($R_c = -8.1$ Å).

Selectivity of the Ammonia-Conducting Channel Toward Water Molecules. Due to the extremely high energetic cost of desolvation, the hydrophobic ammonia-conducting channel of AmtB obviously disfavors the physiologically important cations Na^+ and K^+, whose concentrations are much higher than that of ammonium. However, it is intriguing whether they can occupy the binding site as they can also form π-cation interactions with surrounding aromatic rings. Experiments showed that there is no significant inhibition of the Amt/Mep/Rh proteins by Na^+ and K^+,[17,19] which is further verified by adiabatic free energy calculations.[9] However, it is an open question whether water can go through the channel, considering that oxygen is only slightly more electronegative than nitrogen and H_2O and NH_3 are of comparable dipole moments and sizes. To this end, we computed the free energy profile for the passage of water through the ammonia transport channel. Similar to the calculations of AmtB with ammonia/ammonium, we initiated the MD simulations at $R_c = -20.7$ Å (the initial site for NH_4^+). Figure 10 shows the free energy profile for the transduction of

(39) We thank an anonymous referee for pointing out this issue to us.

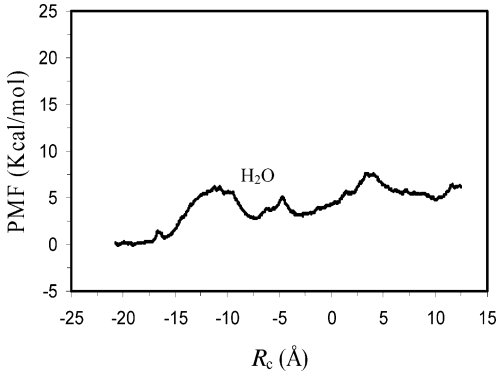

Figure 10. Potential of mean force (PMF) profile for the passage of a water molecule across the AmtB membrane protein.

a water molecule through the AmtB channel. There is no apparent periplasmic binding site for water, in contrast to the case of ammonium. Water requires about 6 kcal/mol to pass the two gates, which rotate to allow the water through. Since the ammonium ion needs only 3.1 kcal/mol to enter the periplasmic binding vestibule, the binding site outside the AmtB channel favors the ammonium ions over water molecules. Once the water molecule enters the channel, however, the energy trajectory is relatively smooth with only low barriers, as the hydrophobic channel can incorporate the hydrogen bond acceptor with not only ammonia but also water using weak interactions with C−H bonds.[9,10] The two highly conserved residues in the mid-membrane center of the pathway, His168 and His318, can interact with water a little more strongly than with ammonia. We note that Khademi et al. investigated the possible water conductivity by AmtB by the measurement of osmotic permeability[40] and the vesicle shrinkage and swelling.[41] Both experiments indicated no additional water conductivity in AmtB proteoliposomes. The structure of AmtB with NH_4^+ also showed no ordered water between the hydrophobic constricted regions of the channel.[10]

Conclusion

We have performed detailed free energy MD simulations on the transduction of ammonium/ammonia through the 20 Å long ammonia-conducting channel of the *Escherichia coli* AmtB membrane protein. In agreement with the analysis of the X-ray structure of AmtB complexed with ammonia or methylamine,[10] simulations revealed a periplasmic binding vestibule which includes Phe107, Trp148, Phe215, and Ser219. This binding vestibule is specific for ammonium ions which form strong noncovalent π-cation interactions with the aromatic rings of Phe107, Trp148, and Phe215. Ser219 plays its role by forming a strong hydrogen bond with NH_4^+. Simulations on the transduction of water indicate that this binding site is not favorable for water molecules which require an activation energy of 6 kcal/mol to go through. For comparison, the activation energy for NH_4^+ is only 3.1 kcal/mol. Of significance, with the entrance of NH_4^+ into the periplasmic binding vestibule, there are remarkable movements of the side chains of surrounding amino acid residues, that is, the flipping of the phenyl ring of Phe107, the slight rotation and shifting of the indole ring of Trp148. These collective conformational changes open a slot for the carboxylate group of Asp160 to access to the solvent. Asp160 normally is buried inside the Amt proteins and forms strong hydrogen bonds with the backbones of Thr165, Gly164, and Gly163 at the N-terminal end of the fifth helix. On the basis of the determined X-ray structures, Khademi et al. claimed that the role of the highly conserved Asp160 is structural. Our simulations showed that, with the opening of the first gate (the phenyl ring of Phe107), the carboxylate group CO_2^- of Asp160 forms hydrogen bonds with the ammonium ion via two water molecules. Thus, the role of Asp160 is functional rather than structural, and Asp160 is actually the proton acceptor from NH_4^+. With the deprotonation of NH_4^+ to NH_3, the second gate (the phenyl ring of Phe215) instantly opens and the subsequent transduction of ammonia through the channel is fairly smooth with only small bumps of less than 3.6 kcal/mol. Figure 11 illustrates the overall ammonium/ammonia transport mechanism in the AmtB membrane protein.

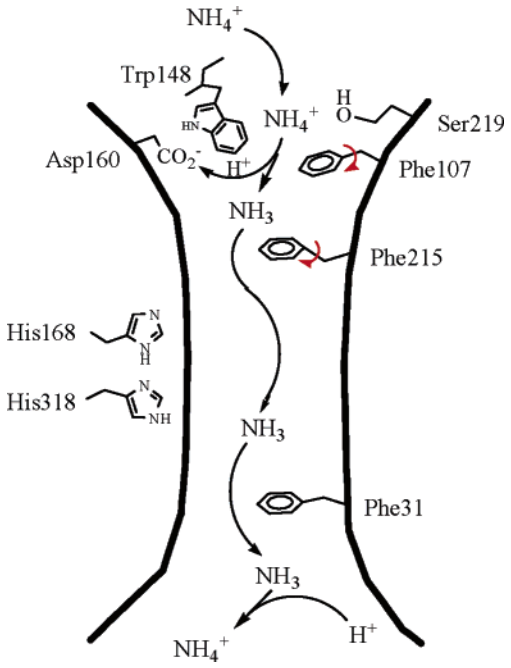

Figure 11. Illustration of the ammonium/ammonia transport mechanism in AmtB. This figure is a modification of the original mechanism proposed by Khademi et al.[10]

Although the ion-binding site at the extracellular pore entry of the AmtB protein is specific for ammonium ions, the barrier for water to pass this site and enter the channel (6 kcal/mol) should be easy to overcome if there is no competition from ammonium ions. Thus, we conclude that water should be able to pass through the AmtB channel alone, but this statement needs further experimental verifications.

Acknowledgment. This work was supported by the Keck Foundation, the National Institutes of Health (NIH), and Western Michigan University.

Supporting Information Available: Complete citation for ref 29 and a snapshot showing the possible protonation of the ammonia on the cytosolic side. This material is available free of charge via the Internet at http://pubs.acs.org.

JA0631549

(40) Priver, N. A.; Rabon, E. C.; Zeidel, M. L. *Biochemistry* **1993**, *32*, 2459−2468.
(41) Fu, D.; Libson, A.; Miercke, L. J. W.; Weitzman, C.; Nollert, P.; Krucinski, J.; Stroud, R. M. *Science* **2000**, *290*, 481−486.